Journal of Photochemistry and Photobiology A: Chemistry 218 (2011) 17–25

Contents lists available at ScienceDirect

Journal of Photochemistry and Photobiology A: Chemistry

journal homepage: www.elsevier.com/locate/jphotochem

Photoinduced energy-transfer and electron-transfer processes in molecules of tetrakis((*E*)-2-(50-hexyl-2,20-bithiophen-5-yl)vinyl)benzene and perylenediimide

Mohamed E. El-Khouly [a,b,*], Dong Hoon Choi [c], Shunichi Fukuzumi [a,d,**]

[a] Department of Material and Life Science, Graduate School of Engineering, Osaka University, Suita, Osaka 565-0871, Japan
[b] Department of Chemistry, Faculty of Science, Kafr ElSheikh University, Kafr ElSheikh 33516, Egypt
[c] Department of Chemistry, Advanced Materials Chemistry Research Center, Korea University, 5 Anam-dong, Sungbuk-gu, Seoul 136-701, Republic of Korea
[d] Department of Bioinspired Science, Ewha Womans University, Seoul 120-750, Republic of Korea

ARTICLE INFO

Article history:
Received 27 July 2010
Received in revised form
15 November 2010
Accepted 25 November 2010
Available online 8 December 2010

Keywords:
Perylenediimide
Oligothiophene
Energy transfer
Electron transfer

ABSTRACT

Photoinduced energy- and electron-transfer processes of donor-σ-acceptor molecules composed of [1,2,4,5-tetrakis((*E*)-2-(50-hexyl-2,20-bithiophen-5-yl)vinyl)benzene] (HPBT) with one, two and four entities of perylenediimide (PDI) forming HPBT–PDI_n (n = 1, 2 and 4) have been examined in this article by utilizing steady-state absorption and emission, computational, electrochemical and time-resolved transient absorption studies. The HPBT–PDI_n molecules are connected through long non-conjugated σ-bonds that may prevent the direct overlap of HPBT and PDI energy levels. Electrochemical studies suggest the exothermic photoinduced electron transfer processes when HPBT and PDI are selectively excited. Upon excitation the HPBT entity, the steady-state emission and femtosecond transient absorption measurements of HPBT–PDI_n revealed an efficient energy transfer from the singlet excited HPBT to PDI with time constants on the order of $\sim 10^{10}$ s^{-1}. The energy donor–acceptor distance, r = ~22 Å, is calculated from the experimental energy transfer rates using Förster theory and from the MO calculations using *ab initio* B3LYP/6-311G method. By selective excitation the PDI entity, the electron-transfer processes take place from HPBT to the singlet excited PDI with time constants on the order of $\sim 10^{8}$ s^{-1}. The slow rates of electron transfer and energy transfer processes indicated that these molecules tend to take conformations with relatively long distance between HPBT and PDI entities.

1. Introduction

Studies on photoinduced energy- and electron transfer in molecular and supramolecular systems have witnessed a rapid growth in the past decades. These studies were aimed to address mechanistic details of light induced processes in chemistry and biology [1–7], and also, to develop molecular optoelectronic devices [8–14]. Incorporation of electron donor and electron acceptor dye molecules within a bulk material may lead to valuable electronic and photonic materials, especially if one or both of the dye manifolds form an interpenetrating network in which photogenerated charge carriers exhibit high mobility. Toward this goal, several organic compounds have been applied to construct molecular devices. Among them, perylenediimides (PDIs) have been employed in various molecular systems with efficient energy- and electron-transfer functionalities because of its excellent photophysical and photochemical properties such as the high fluorescence quantum yield, the large absorption band at around 550 nm, the high electron-acceptor ability in its excited state, high stability against environmental influences, and easy accessibility [15–25]. Due to these features, PDIs have been used as industrial pigments and dyes [26] and as active components in photovoltaic cells [27–30]. The ability to form nanometer-size aggregates is also an interesting property of PDI [31–33]. Most importantly, PDIs are outstanding n-type organic semiconductors [31,34,35]. Thus combination of electron-donating chromophores with electron-accepting PDIs will lead to interesting heterojunction materials [36]. Among these materials, oligothiophenes are viewed as ideal materials for organic molecular devices [37–39], OLEDs [40], chemosensors [41], biosensors [42], and electrochromic devices [43], since they are electron rich and provide as outstanding ability

* Corresponding author at: Department of Material and Life Science, Graduate School of Engineering, Osaka University, Suita, Osaka 565-0871, Japan. Tel.: +81 6 6879 7369; fax: +81 6 6879 7370.
** Corresponding author at: Department of Material and Life Science, Graduate School of Engineering, Osaka University, Suita, Osaka 565-0871, Japan. Tel.: +81 6 6879 7368; fax: +81 6 6879 7370.
E-mail addresses: mohamedelkhouly@yahoo.com (M.E. El-Khouly), fukuzumi@chem.eng.osaka-u.ac.jp (S. Fukuzumi).

1010-6030/$ – see front matter © 2010 Elsevier B.V. All rights reserved.
doi:10.1016/j.jphotochem.2010.11.018

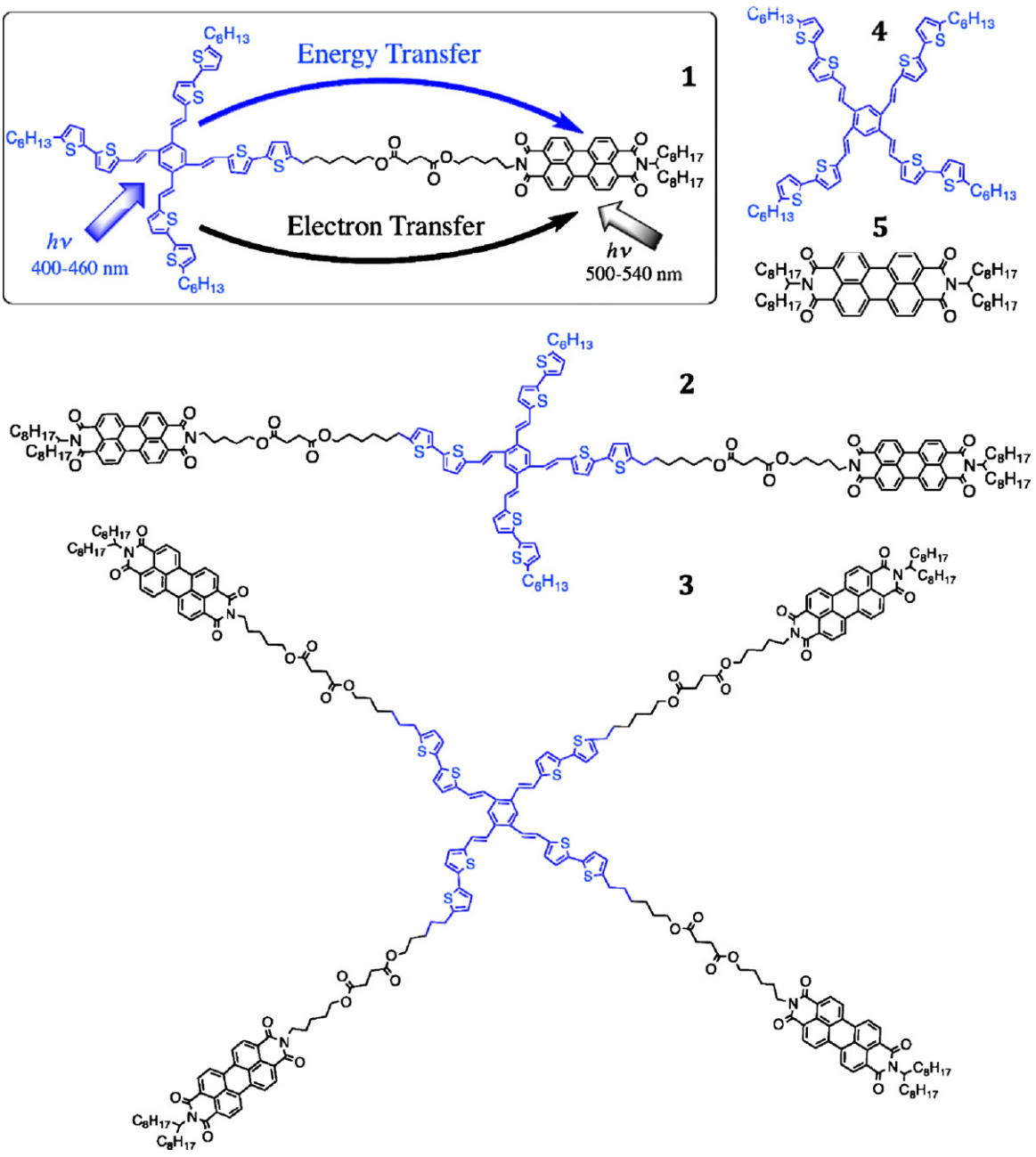

Fig. 1. Molecular structures of HPBT–PDI$_n$ (**1**–**3**) and the references **4** and **5**.

to acquire positive charges and to transport them through self-assembled monolayers [44–46].

In the last decade, several perylenediimide/oligothiophene molecules have been tested in solar cell applications [47–54]. However, to the best of our knowledge, the details of photoinduced intramolecular and intermolecular processes of molecules composed of oligothiophenes/perylenediimides are rare in the literature [55–59]. We report herein the photoinduced energy- and electron-transfer reactions of [1,2,4,5-tetrakis((*E*)-2-(50-hexyl-2,20-bithiophen-5-yl)vinyl)-benzene] (HPBT) that is covalently linked with one, two and four entities of perylenediimides (PDIs) to form HPBT–PDI (**1**), HPBT–PDI$_2$ (**2**), and HPBT–PDI$_4$ (**3**), respectively (Fig. 1). The long s linkers were employed to make these two moieties separate to show their independent electronic and photophysical properties, claiming to be a good model for the study of energy- and electron-transfer processes in dual function semiconductors. Quite recently, Choi and co-workers reported that the examined HPBT–PDI$_n$ compounds were appreciable for construct photovoltaic device [54]. In order to get clear picture about the photoinduced intramolecular and intermolecular processes between the HPBT and PDI components, we examined these materials by using steady-state absorption and emission, electrochemistry, femtosecond and nanosecond laser photolysis techniques.

2. Experimental

2.1. Materials

The examined semiconducting HPBT–PDI$_n$ molecules were synthesized according to previously reported procedures by Choi and co-workers [54].

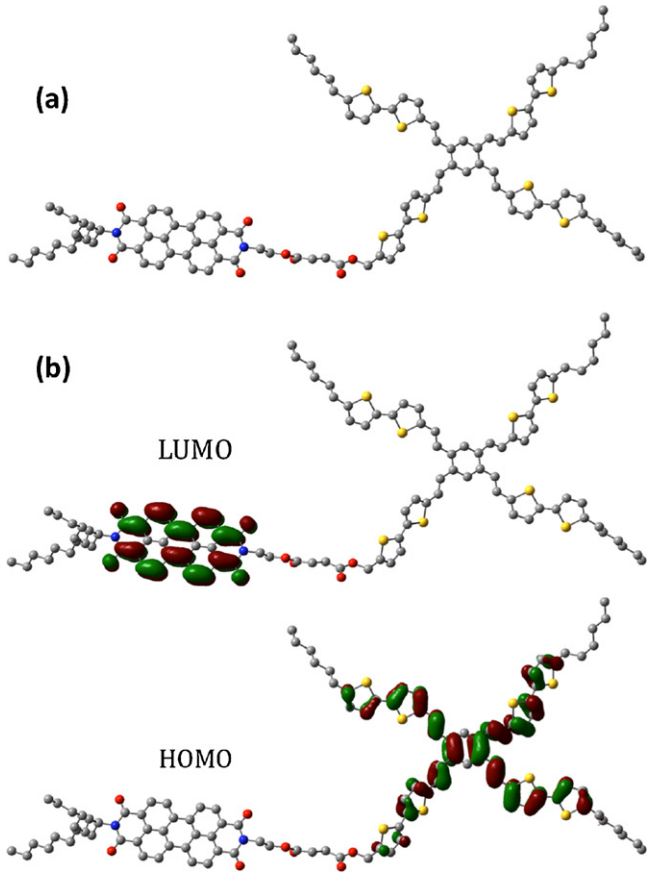

Fig. 2. (a) *Ab initio* B3LYP/6-311G optimized structure (ball- and stick model) and (b) frontier HOMO and LUMO orbitals of the HPBT–PDI dyad.

2.2. Instruments

Steady-state absorption spectra were recorded on a Shimadzu UV-3100PC spectrometer or a Hewlett Packard 8453 diode array spectrophotometer at room temperature. Fluorescence measurements were carried out on a Shimadzu spectrofluorophotometer (RF-5300PC). Phosphorescence spectra were obtained by a SPEX fluorolog τ3 spectrophotometer. Emission spectra in the NIR region were detected by using a Hamamatsu Photonics R5509-72 photomultiplier. An argon-saturated 2-methyltetrahydrofuran (2-MeTHF) solution containing HPBT and PDI at 77 K was excited indicated wavelengths. The fluorescence lifetimes were measured by a Photon Technology International GL-3300 with a Photon Technology International GL-302, nitrogen laser/pumped dye laser system, equipped with a four-channel digital delay/pulse generator (Stanford Research System Inc. DG535) and a motor driver (Photon Technology International MD-5020). The excitation wavelength was 530 nm (for PDI reference and **1**–**3**) and 420 nm (for HPBT reference).

Density-functional theory (DFT) calculations were performed on a COMPAQ DS20E computer. Geometry optimizations were carried out using the Becke3LYP functional and 6-311G basis set, with the unrestricted Hartree–Fock (UHF) formalism and as implemented in the *Gaussian 09* programs Rev. A.02. Graphical outputs of the computational results were generated with the *Gauss View* software program (ver. 5) developed by Semichem, Inc.

Electrochemical measurements were performed on an ALS630B electrochemical analyzer in deaerated benzonitrile containing tetra-*n*-butylammonium hexafluorophosphate ($TBAPF_6$; 0.10 M) as supporting electrolyte at 298 K. A conventional three-electrode cell was used with a platinum working electrode (surface area of 0.3 mm^2) and a platinum wire as the counter electrode. The Pt working electrode was routinely polished with BAS polishing alumina suspension and rinsed with acetone before use. The measured potentials were recorded with respect to SCE reference electrode. All electrochemical measurements were carried out under an atmospheric pressure of argon.

Femtosecond transient absorption spectroscopy experiments were conducted using an ultrafast source: Integra-C (Quantronix Corp.), an optical parametric amplifier: TOPAS (Light Conversion Ltd.) and a commercially available optical detection system: Helios provided by Ultrafast Systems LLC. The source for the pump and probe pulses were derived from the fundamental output of Integra-C (780 nm, 2 mJ/pulse and fwhm = 130 fs) at a repetition rate of 1 kHz. 75% of the fundamental output of the laser was introduced into TOPAS which has optical frequency mixers resulting in tunable range from 285 nm to 1660 nm, while the rest of the output was used for white light generation. Typically, 2500 excitation pulses were averaged for 5 s to obtain the transient spectrum at a set delay time. Kinetic traces at appropriate wavelengths were assembled from the time-resolved spectral data. All measurements were conducted at 298 K. The transient spectra were recorded using fresh solutions in each laser excitation. For nanosecond transient absorption measurements, deaerated solutions of the compounds were excited by a Panther OPO equipped with a Nd:YAG laser (Continuum, SLII-10, 4–6 ns fwhm) with a power of 10–15 mJ per pulse. The photochemical reactions were monitored by continuous exposure to a Xe lamp (150 W) as a probe light and a photomultiplier tube (Hamamatsu 2949) as a detector. Solutions were

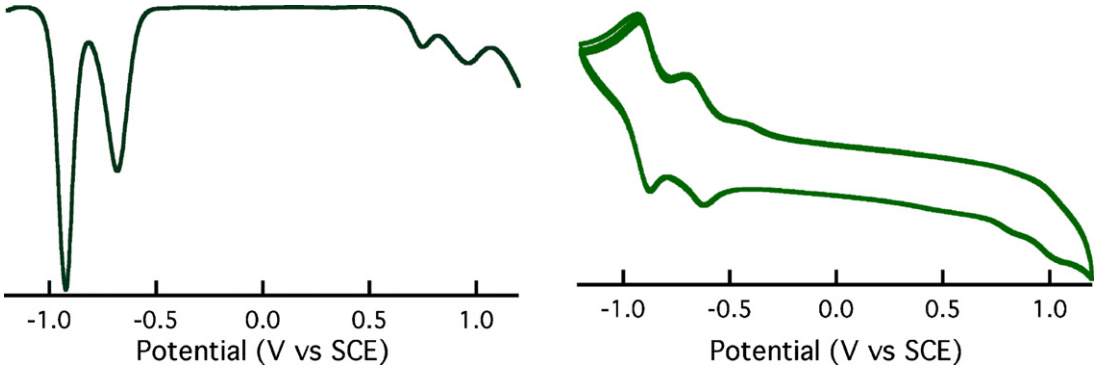

Fig. 3. DPV (left) and CV (right) voltammograms of **2** in deaerated benzonitrile. Scan rate = 50 mV/s.

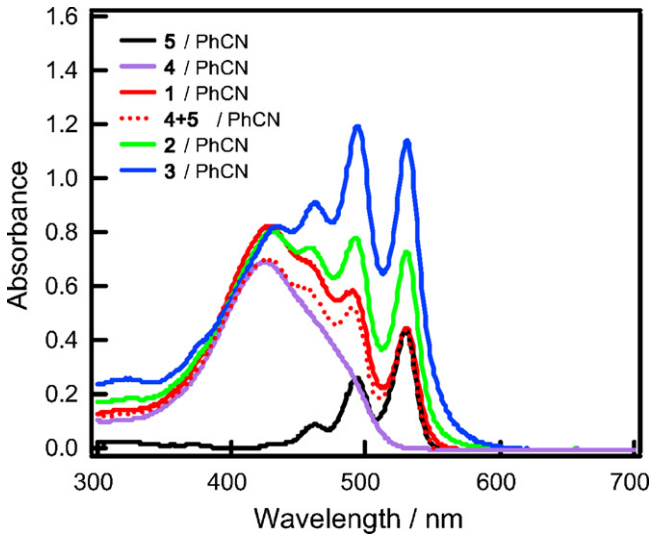

Fig. 4. Steady-state absorption spectra of the studied compounds **1**–**5** (6.89 μM) in benzonitrile.

deoxygenated by argon purging for 15 min prior to the measurements.

3. Results and discussion

3.1. Characterization

The thermal properties of compounds **1**–**3** were characterized by thermogravimetric analysis (TGA) and differential scanning calorimetry (DSC). TGA measurements revealed good thermal stability, where the decomposition temperatures were found to be 389–391 °C. In DSC thermograms, **1** and **2** exhibited a distinct crystalline-isotropic transition at 140 and 117 °C, respectively. The crystallization temperatures of **1** and **2** were also observed at 1 1 1 and 87 °C, respectively, during the cooling cycle. In contrast, **3** did not show a crystalline melting temperature, but it did show a glass transition temperature at 75 °C only, indicating its amorphous nature.

3.2. Computational studies

In the studied molecule **1**, HPBT and PDI are connected with the flexible linker that facilitate conformation variations in terms of distances and relative orientations between the donor and acceptor entities in solution. To identify the most probable conformation of the compound **1** in solution, the structural energy minimization using density functional methods (DFT) at the B3LYP/6-311G level. Among the possible conformations, the optimized structure (Fig. 2a) showed that the center-to-center distance (d_{CC}) between the PDI and HPBT is 25.55 Å, while the edge-to-edge distance was found to be 12.06 Å.

The energies and electronic wave function distributions for the frontier molecular orbitals (MOs) clearly demonstrate predominant contributions of the HPBT in the highest occupied molecular orbital (HOMO) and those of the PDI entity in the lowest unoccupied molecular orbital (LUMO) (Fig. 2b), validating the preferred photoinduced electron transfer direction from HPBT to PDI yielding the radical–ion pair ($HPBT^{\bullet+}$–$PDI^{\bullet-}$). The absence of HOMO and LUMO over the PDI and HPBT, respectively, indicating weak charge-transfer interactions between the HPBT and PDI entities in the ground state.

3.3. Electrochemical studies

Cyclic voltammetry (CV) and differential pulse voltammetry (DPV) measurements were performed as a means to clarify electrochemical properties of **1**–**3** and the references. **4** and **5** (Fig. 3 and Figs. S1 and S2 in the Supporting Information). All measurements were carried out in benzonitrile containing tetra-*n*-butylammonium hexafluorophosphate ($TBAPF_6$; 0.10 M) at room temperature. The first reduction potentials (E_{red}) of PDI were recorded at −672, −688 and −688 mV vs SCE for **1**, **2** and **3**, respectively. Scanning to positive potentials, the HPBT moiety undergoes one-electron oxidation (E_{ox}) at 740, 752 and 736 mV vs SCE. The driving forces of the electron-transfer process, ΔG_{ET}, can be estimated from the Eq. (1) [60]:

$$\Delta G_{ET} = E_{ox} - E_{red} - \Delta E_{00} + \Delta G_s \quad (1)$$

where ΔE_{00}, E_{ox} and E_{red} are the excitation energy, oxidation potential of HPBT and reduction potential of PDI, respectively. ΔG_s refers to the static Coulomb energy, calculated by using the "dielectric continuum model" [61] according to Eq. (2):

$$\Delta G_s = \frac{e_2}{4\pi} \cdot \varepsilon_0 \cdot \varepsilon_s \cdot d_{cc} \quad (2)$$

The center-to-center distance, d_{CC}, was calculated for the optimized structure in Fig. 2 to be 27.72 Å. The symbols ε_0 and ε_s represent vacuum permittivity and dielectric constant of solvent used for photochemical and electrochemical studies, respectively.

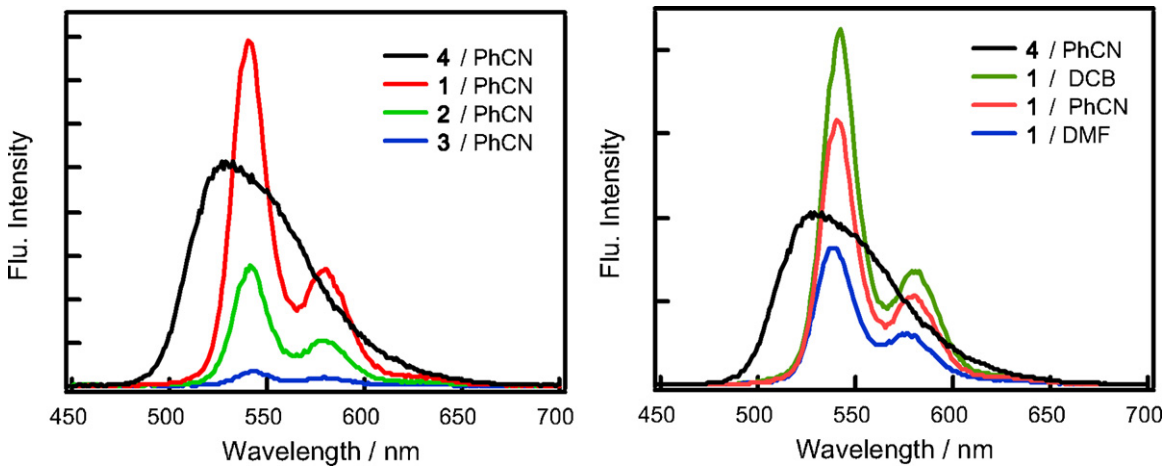

Fig. 5. (Left) Emission spectra of **1**–**3** and the reference compound **4** in benzonitrile (6.89 mM); λ_{ex} = 410 nm. (Right) Emission spectra of 1 in different solvents and the reference compound 4.

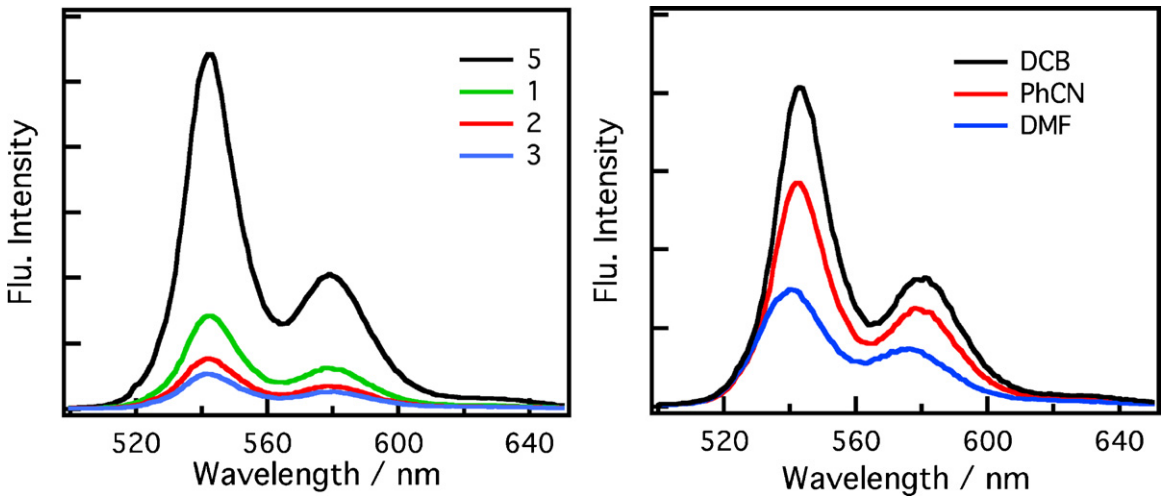

Fig. 6. Emission spectra of **1**–**5** in PhCN (left) and **1** in different solvents (right); λ_{ex} = 525 nm.

From Eq. (2), the Coulombic term depending on the solvent polarity and donor–acceptor distance and tends to become negligibly small when distance becomes larger and in polar solvents. The $-\Delta G_{ET}$ values via the singlet excited PDI (2.34 eV) in benzonitrile were estimated to be 0.87, 0.84, 0.86 eV for **1**, **2** and **3**, respectively. By changing the solvents to *o*-dichlorobenzene (DCB) and dimethylformamide (DMF), the $-\Delta G_{ET}$ values of 1 via the singlet excited PDI were found to be 0.79 and 0.93, respectively. In general, the negative ΔG_{ET} values suggest that the electron transfer via the singlet excited PDI are thermodynamically feasible in polar and less polar solvents.

The $-\Delta G_{ET}$ values via the singlet excited HPBT (2.56 eV) were also estimated to be 1.09, 1.06, 1.07 eV for **1**, **2** and **3**, respectively. However, the energy transfers from the singlet excited HPBT (2.56 eV) to that of PDI (2.34 eV) is anticipated as will describe in the forthcoming sections.

3.4. Steady-state absorption studies

Steady-state absorption spectra of the **1**–**3** molecules along with those of the reference compounds perylenediimide (PDI) and oligothiophene (HPBT) in benzonitrile at room temperature are depicted in Fig. 4. The solution of PDI **5** showed the lowest energy absorption band at 530 nm with two vibronic bands at 490 and 463 nm. These features remain almost identical in the compounds **1**–**3**, where the 530 nm band originating from the PDI blocks shifts to red only by 1 nm relative to that of the reference compound PDI. The reference compound HPBT **4** has a broad absorption band with a maximum at 424 nm, corresponding to the p–p* transition of the conjugated oligothiophene backbone in solution. The absorption spectrum of the **1** can be reconstructed by a summation from those of the reference compounds PDI and HPBT with a 1:1 ratio. This is a clear evidence for weak electronic interactions between HPBT and PDI. In other words, the electron donor and acceptor retain their separate electronic structural entities in the **1**–**3** molecules.

3.5. Photophysical studies of the covalently linked HPBT–PDI_n

The photophysical behavior of **1**–**3** was first investigated using steady-state fluorescence in benzonitrile. By exciting the HPBT entity with 410 nm excitation light, the broad emission of the singlet excited HPBT was observed at 528 nm (Fig. 5), of which the

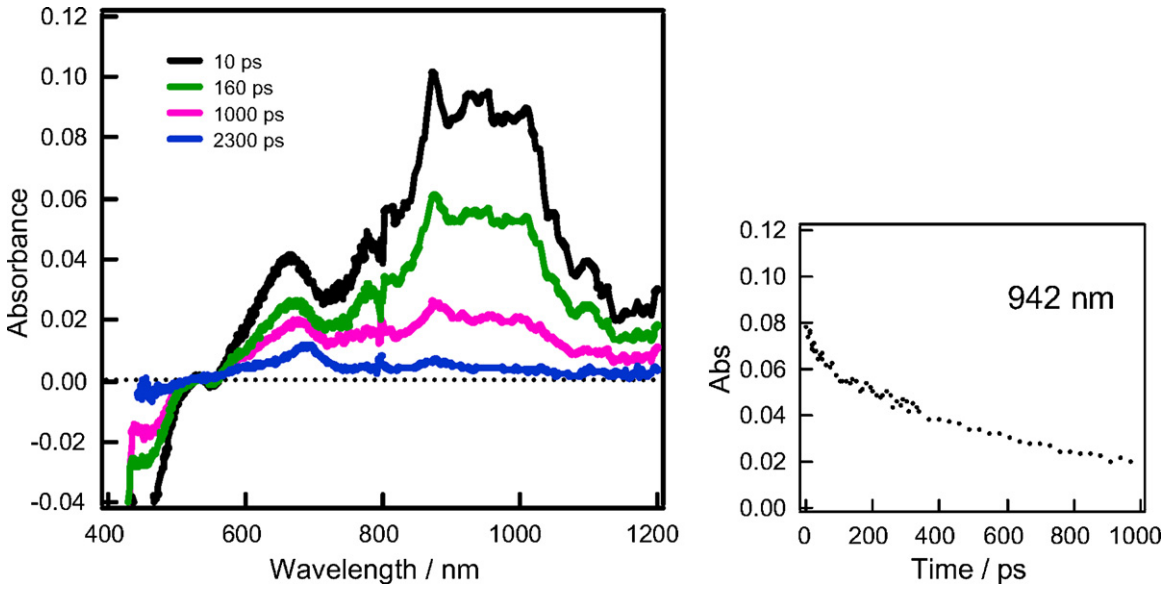

Fig. 7. Femtosecond transient absorption spectra of HPBT **4** in deaerated benzonitrile after the laser excitation at 430 nm.

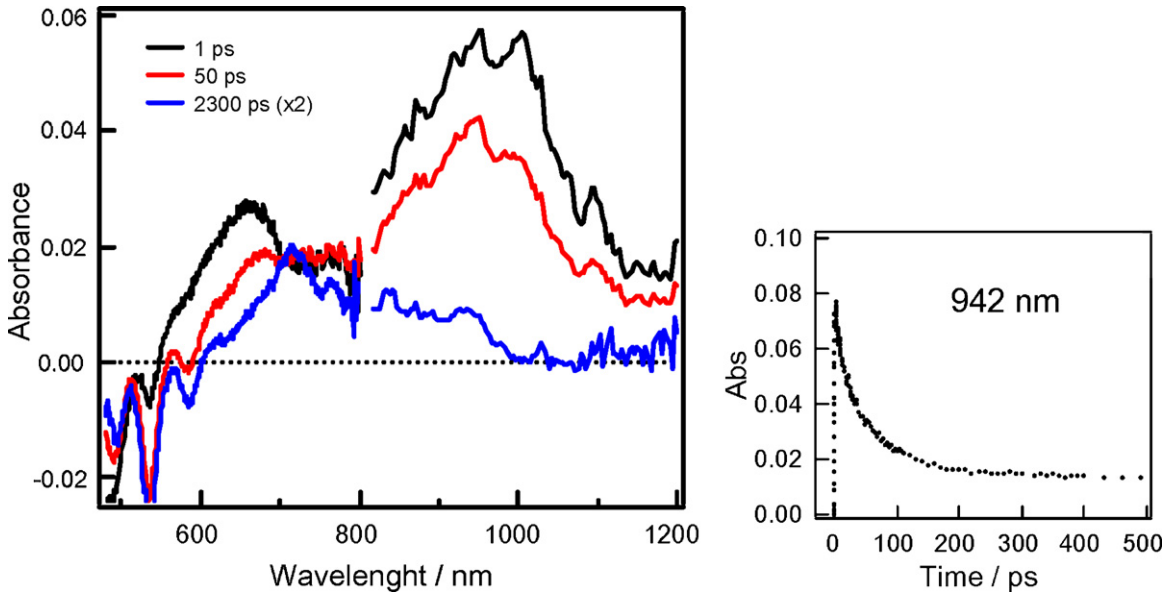

Fig. 8. Femtosecond transient absorption spectra of **1** in deaerated benzonitrile after the laser excitation at 430 nm.

quantum yield was evaluated as 0.18. In case of **1**–**3**, the emission occurs exclusively from the PDI (539 and 580 nm) even though the excitation light (λ_{ex} = 410 nm) is absorbed primarily by the HPBT component. This observation is indicative of efficient ENT from the singlet excited HPBT (2.56 eV) to that of PDI (2.34 eV). The fluorescence intensities of the formed PDI were found to decrease upon increasing the number of PDI units. By changing the solvent to *o*-dichlorobenzene and dimethylformamide, same features were observed as that in benzonitrile. The only difference is that the emission of the formed singlet PDI decreases with increasing the polarity of solvents.

It is readily observed that the emission spectrum of HPBT and the absorption spectrum of PDI are favorably overlapped, which enables efficient Förster energy transfer (Fig. S3 in the Supporting Information). Excitation spectra of HPBT–PDI$_n$, recorded by fixing the emission monochromator to the PDI emission maximum in the range of 540 nm, revealed spectrum with the HPBT absorption (Fig. S4 in the Supporting Information). This observation confirms that the observed PDI emission is a result of singlet ENT from the HPBT entity to PDI.

The intense emission band of the reference compound PDI (λ_{ex} = 525 nm) shows two vibronic features (at 540 and 580 nm) that are mirror images of its absorption spectrum [15–25,62]. When the PDI moiety of **1**–**3** is selectively excited (λ_{ex} = 525 nm), the fluorescence intensity of the PDI entity showed significant quenching compared to that of PDI **5** (Fig. 6, left). The quantum-yields of the singlet excited PDI were evaluated as 0.13 (**1**), 0.06 (**2**) and 0.05 (**3**), which is significantly lower compared with that of **5** (0.88). Because the singlet state of PDI is lower than that of HPBT, energy transfer from HPBT to PDI cannot occur in the **1**–**3** when the PDI is selectively excited. Thus, it is indicated that ET from HPBT to the singlet excited PDI occurred in **1**–**3**.

In the case of **1**–**3**, the PDI emission bands are quenched by ca. 60% (**1**), 82% (**2**) and 95% (**3**) compared with the emission intensity of PDI **5**. Basically, the fluorescence quenching of the singlet PDI of **1**–**3** is due to the electron transfer from HPBT to the singlet PDI. The higher quenching of **2** and **3** compared to **1** may rationalize by existing different conformations with different distances between the HPBT and PDI entities. The finding that the quenching of HPBT–^{1}PDI$_n$* increases with increasing the polarities of solvent also indicates the electron-transfer character of the quenching process of the singlet excited PDI (Fig. 6, right) [63].

The fluorescence lifetime measurements track the above considerations in a more quantitative way, giving kinetic data of the electron transfer processes in polar benzonitrile. The fluorescence decay-profiles of the singlet excited PDI of the investigated compounds **1**–**3** showed substantial quenching of the fluorescence lifetimes (3.12 ns (**1**), 2.66 ns (**2**) and 2.55 ns (**3**)) compared to that of PDI reference **5** (6.00 ns). Based on the short lifetimes, the rates (k_{ET}) and quantum yields (Φ_{ET}) for the electron transfer processes were evaluated as 1.54×10^8 s^{-1} and 0.48 (**1**), 2.09×10^8 s^{-1} and 0.56 (**2**), and 2.25×10^8 s^{-1} and 0.57 (**3**) [64]. By changing the solvent to *o*-dichlorobenzene and dimethylformamide, the k_{ET} and Φ_{ET} values of 1 were estimated as 2.08×10^8 and 0.55 (DMF), and 1.43×10^8 and 0.46 (DCB). From these values, it can be pointed out that the k_{ET} became faster with an increase in the solvent polarity.

Upon exciting the HPBT entity, the singlet excited HPBT **5** revealed a mono-exponential decay with a lifetime of 2.00 ns in benzonitrile. It was difficult to follow the energy transfer from the singlet HPBT to PDI of **1**–**3** because the decays of the singlet HPBT are too fast to be detected by our instrument limitation.

For this, we performed the femtosecond laser measurements by using 430 nm laser excitation to examine the photoinduced singlet-singlet energy-transfer processes from the singlet excited HPBT to PDI of **1**–**3**. Photons at this wavelength exclusively pump the HPBT component, but not the PDI due to the low extinction coefficient of PDI at this wavelength. The transient spectra of HPBT **4** showed broad absorption in the visible and NIR region that assigned to the singlet excited state of HPBT, which decayed with a first-order rate constant of 8.3×10^8 s^{-1} (Fig. 7). At 2300 ps, one can notice the formation of a new absorption band at 690 nm that assigned to the triplet state of the triplet HPBT, as we will describe in the forthcoming sections. When turning to **1**–**3**, the singlet HPBT generated immediately after the laser excitation donates its singlet energy to PDI (Fig. 8 and Fig. S5 in the Supporting Information). The ENT process is confirmed by the formation of the singlet PDI at 530 nm within 50 ps after the laser excitation, which agrees with the initial decay of the singlet HPBT. The decay rates of the singlet excited HPBT of **1**–**3** were found to be 3.00×10^{10} s^{-1} (**1**), 3.80×10^{10} s^{-1} (**2**), and 2.60×10^{10} s^{-1} (**3**), which are much faster

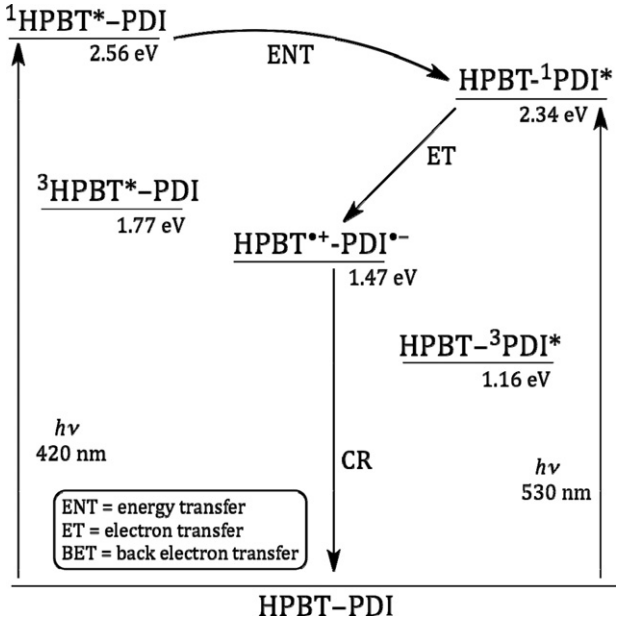

Fig. 9. Energy level diagram of HPBT–PDI in benzonitrile via the singlet excited HPBT and PDI.

than that of **4** (6.0×10^8 s^{-1}). From these values, the k_{ENT} from the singlet excited HPBT to PDI were found to be 2.95×10^{10} s^{-1} (**1**), 3.75×10^{10} s^{-1} (**2**), and 2.55×10^{10} s^{-1} (**3**). Based on the (k_{ENT}), the quantum yields of the energy-transfer (Φ_{ENT}) were determined to be 0.98, 0.99 and 0.98 for **1**, **2** and **3**, respectively. It is worth mention that these values are slower than the k_{ENT} values of the reported pentathiophene-perylene with a long flexible alkyl linker (5T-$(CH_2)_6$-PDI) ($k_{ENT} = 1.0 \times 10^{12}$ s^{-1}) [55].

After the energy transfer is completed, electron transfer from HPBT to the singlet PDI becomes possible. At 2300 ps, one could notice absorption bands at 716, 760 and 950 nm that assigned to the formation of the PDI radical anion by comparison with the spectrum produced by the one-electron reduction of PDI with tetrakis(dimethylamino)ethylene (Fig. S6 in the Supporting Information).

By using the experimentally obtained k_{ENT}, an effective interaction radius between the electron-donating HPBT and electron-accepting PDI can be calculated [17,65–67]. It is known that the k_{ENT} depends on the extent of spectral overlap of the emission spectrum of the donor with the absorption spectrum of the acceptor, the quantum yield of the donor, the relative orientation of the donor and acceptor transition dipoles, and the distance between the donor and acceptor molecules [66]. Because we think that there is a Förster type energy transfer, the distance between donor (D) and acceptor (A) plays an important role. The k_{ENT} from a donor to acceptor is given by Eq. (3)

$$k_{ENT} = {\tau_D}^{-1} \cdot \left(\frac{R_0}{r}\right)^6 \quad (3)$$

where τ_D is fluorescence lifetime of HPBT **5**, r is the distance between donor and acceptor, and R_0 is the Förster distance (the distance at which energy transfer is 50% efficient and is typically in the range of 20–60 Å.). To calculate the Förster distance, R_0, the simplified Eq. (4) can be used

$$R_0^6 = 8.79 \times 10^{23} \cdot k^2 \cdot n^{-4} \cdot \Phi_D \cdot J(\lambda) \quad (4)$$

where k^2 is the orientation factor, and generally assumed as 2/3 in calculations, n is the refractive index of the medium, Φ_D is the quantum yield of the donor in the absence of acceptor, and $J(\lambda)$ is the overlap integral calculated from the acceptor absorption spectrum and the fluorescence spectrum of the donor, with the total intensity normalized to unity. Once R_0 is calculated from these experimentally known values, the distance between donor and acceptor can be easily obtained. Knowing the values of R_0 (44.77 Å), τ_D (2 ns), and $J(\lambda)$ (4.15×10^{15} M^{-1} cm^{-1} nm^4), the donor–acceptor distance (r) can be calculated by using Eq. (1) as 22.2 Å. This value is in an agreement with that estimated from the optimized structure (Fig. 2). The long r may explain the slower k_{ET} and k_{ENT} values of the examined compounds compared with the reported pentathiophene-perylene with a flexible alkyl linker (5T-$(CH_2)_6$-PDI) ($k_{ENT} = \sim 10^{12}$ s^{-1} and $k_{ET} = \sim 10^{11}$ s^{-1}) [55]. The fast k_{ENT} and k_{ET} values in (5T-$(CH_2)_6$-PDI) were rationalized by the folded structure ($r = 5.3$ Å).

The complementary nanosecond transient spectra of **1**–**3** obtained by 430 nm laser excitation in benzonitrile showed no characteristic absorption bands of the radical–ion pairs (Fig. S7 in the Supporting Information). This observation indicates that the charge-recombination between HPBT$^{\bullet+}$ and PDI$^{\bullet-}$ is rapid to be detecting in the microsecond time region. The absence of the characteristic absorption bands of the triplet HPBT or triplet PDI indicates that the radical–ion pairs recombined to populate the ground state.

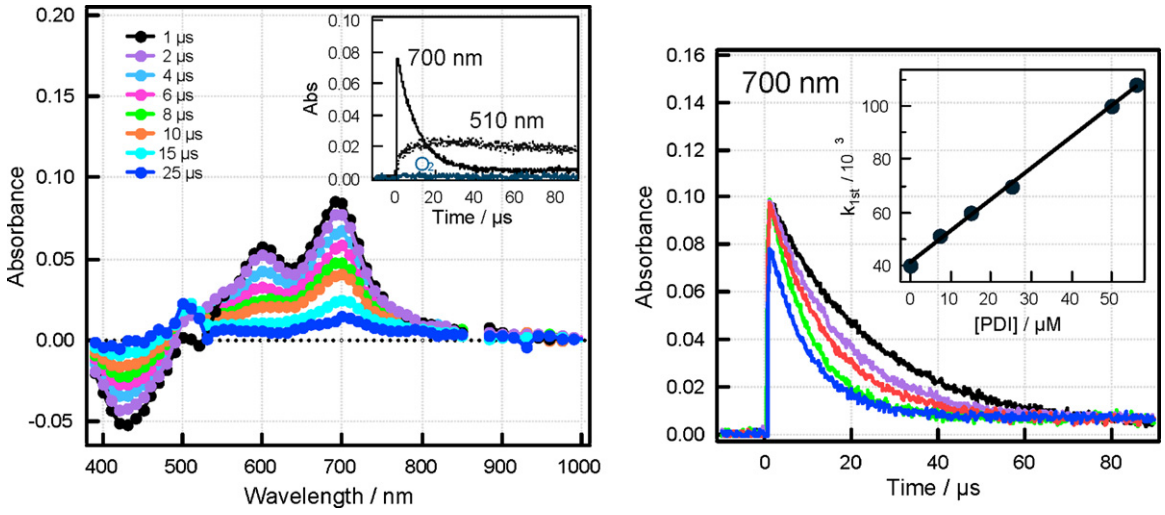

Fig. 10. (Left) Nanosecond transient spectra of HPBT **4** (0.03 mM) in the presence of PDI **5** (0.05 mM) in deaerated benzonitrile after the laser excitation at 430 nm. (Right) Decay–time profiles of the triplet HPBT at 700 nm with changing the concentrations of PDI in deaerated benzonitrile.

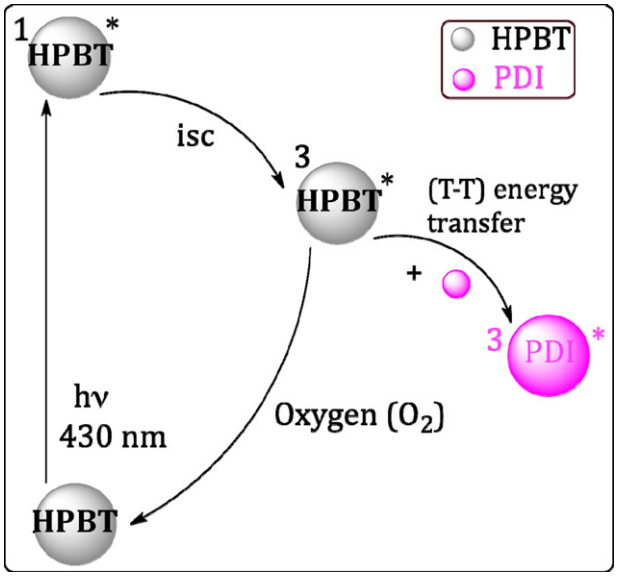

Fig. 11. Intermolecular reactions between HPBT and PDI in the studied solvents (λ_{ex} = 430 nm).

Fig. 9 shows the energy-level diagram summarizing the observed intramolecular events of HPBT–PDI$_n$. Upon photoirradiation of **1**–**3** by 430 nm laser excitation, the singlet excited HPBT decayed by energy transfer to populate the singlet PDI. The efficient energy transfer is followed by electron transfers from HPBT to the singlet excited PDI to form the radical–ion pair HPBT$^{\bullet+}$–PDI$^{\bullet-}$. Finally, the radical–ion pair relaxes to its ground state, because formation of the triplet excited PDI is not efficient for **1**–**3**.

3.6. Photochemical reaction between HPBT and PDI

Nanosecond laser flash photolysis of HPBT **4** (0.03 mM) with 430 nm laser light in deaerated benzonitrile produced the transient absorption spectra in the vis/NIR region with a maximum at 700 nm that corresponds to the triplet excited HPBT (Fig. S8 in the Supporting Information), which populated via the intersystem crossing process from the singlet excited HPBT. The decay of the triplet-excited state of HPBT was found to be 4.0×10^4 s^{-1}. By photoexcitation of HPBT (0.03 mM) in the presence of PDI (0.03–0.10 mM) in argon-saturated benzonitrile using 430 nm laser photolysis, the transient spectra exhibit the characteristic band of triplet-excited state of HPBT (^{3}HPBT*) at 700 nm. With the decay of ^{3}HPBT*, the concomitant rise at 510 nm was observed that corresponds to the triplet excited PDI (Fig. 10 and Figs. S9 and S10 in the Supporting Information). The decay rate of the triplet HPBT was found to be 1.9×10^5 s^{-1}, which is comparable to the formation of triplet PDI (1.8×10^5 s^{-1}). These observations suggest the triplet–triplet energy-transfer process from the HPBT to PDI. We find through phosphorescence measurements that the energy level of the triplet HPBT lies at 1.77 eV (Fig. S11 in the Supporting Information), well lower the triplet PDI (1.16 eV) [62]. It should be noted here that the radical species of both HPBT and PDI are not detected via the triplet excited HPBT, indicating the absence of electron-transfer reactions in such combination.

The effects of the concentrations of PDIs on the kinetic behavior of transient species are studied (Fig. 10). It is evident that the decay-rates of triplet HPBT are significantly increased with increasing [PDI]. Form the analysis of the data in terms of the single exponential decays, the rate constant of the energy-transfer process was estimated to be 2.0×10^9 M^{-1} s^{-1}. It should be mentioned here that such energy transfer from the triplet excited HPBT to PDI was suppressed in oxygen-saturated solution, owing to energy transfer from ^{3}HPBT* to the low-lying triplet oxygen. The intermolecular reactions between HPBT and PDI in the presence and absence of oxygen can be summarized as in Fig. 11.

By changing the solvent to toluene and *o*-dichlorobenzene, the obtained nanosecond transient spectra by 430 nm laser excitation of the HPBT/PDI mixture are similar to that of benzonitrile (Figs. S12 and S13 in the Supporting Information). The k_{ENT} values were found to be 3.2×10^9 M^{-1} s^{-1} (TN) and 1.7×10^9 M^{-1} s^{-1} (*o*-DCB). The finding that the quenching rates of the triplet excited HPBT increase with the decrease of the refractive index (ε = 1.496 (TN), 1.528 (PhCN), 1.55 (*o*-DCB)) confirming the occurrence of energy transfer from the triplet HPBT to the triplet PDI.

4. Conclusion

Photoinduced intramolecular energy- and electron-transfer processes of donor-σ-acceptor molecules bearing the cruciform p-type HPBT molecule with one, two and four entities of PDI forming HPBT–PDI$_n$ (n = 1, 2 and 4) have been studied in this paper. The absorption of HPBT covers the wavelength region where absorption of PDI has minima. When the HPBT moiety was selectively excited by 430 nm laser light, efficient energy transfer from the singlet excited HPBT to PDI was clearly observed indicating that HPBT acts as an antenna of the ET system. The steady-state emission, computational, electrochemical, fluorescence lifetime and femtosecond transient absorption studies showed the electron transfer from HPBT to the singlet excited PDI. The slow rates of energy-transfer and electron-transfer processes can be attributed to the longer distance between PDI and HPBT entities (~22 Å). The photochemical behavior of mixture system of HPBT and PDI showed different features compared with that of the HPBT–PDI$_n$ connected systems. The nanosecond studies showed the energy transfer from the triplet excited HPBT to the low-lying triplet PDI.

Acknowledgments

This work was partially supported by the Global COE (center of excellence) program "Global Education and Research Center for Bio-Environmental Chemistry" of Osaka University from Ministry of Education, Culture, Sports, Science and Technology (MEXT), Japan.

Appendix A. Supplementary data

Supplementary data associated with this article can be found, in the online version, at doi:10.1016/j.jphotochem.2010.11.018.

References

[1] R.E. Blankenship (Ed.), Molecular Mechanisms of Photosynthesis, Blackwell Science, Oxford, U.K., 2002.
[2] T. Brixner, J. Stenger, H.M. Vaswani, M. Cho, R.E. Blankenship, G.R. Fleming, Nature 434 (2005) 625.
[3] B.A. Heller, D. Holten, C. Kirmaier, Science 269 (1995) 940.
[4] M.R. Wasielewski, Chem. Rev. 92 (1992) 435.
[5] A.F. Collings, C. Critchley (Eds.), Artificial Photosynthesis, from Basic Biology to Industrial Application, Wiley-VCH, Weinheim, 2005.
[6] D. Gust, T.A. Moore, A.L. Moore, Acc. Chem. Res. 42 (2009) 1890.
[7] H. Imahori, D.M. Guldi, K. Tamaki, Y. Yoshida, C. Luo, Y. Sakata, S. Fukuzumi, J. Am. Chem. Soc. 123 (2001) 6617.
[8] C.J. Brabec, N.S. Sariciftci, J.C. Hummelen, Adv. Funct. Mater. 11 (2001) 15.
[9] G. Yu, J. Gao, J.C. Hummelen, F. Wudl, A.J. Heeger, Science 270 (1995) 1789.
[10] M.C. Petty, M.R. Bryce, D. Bloor (Eds.), Introduction of Molecular Electronics, Oxford University Press, New York, 1995, p. 2001.
[11] M. Granstrom, K. Petrisch, A.C. Arias, A. Lux, M.R. Andersson, R.H. Friend, Nature 395 (1998) 257.
[12] J.J.M. Halls, C.A. Walsh, N.C. Greenham, E.A. Marseglia, R.H. Friend, S.C. Moratti, A.B. Holmes, Nature 376 (1995) 498.

[13] D. Chirvase, J. Parisi, J.C. Hummelen, V. Dyakonov, Nanotechnology 15 (2004) 1317.
[14] C.D. Dimitrakopoulos, P.R.L. Malenfant, Adv. Mater. 14 (2002) 99.
[15] R.D. Costa, F.J. Céspedes-Guirao, E. Ortí, H.J. Bolink, J. Gierschner, F. Fernández-Lázaro, A. Sastre-Santos, Chem. Commun. (2009) 3886.
[16] R.H. Goldsmith, L.E. Sinks, R.F. Kelley, L.J. Betzen, W. Liu, E.A. Weiss, M.A. Ratner, M.R. Wasielewski, Proc. Natl. Acad. Sci. 102 (2005) 3540.
[17] B.K. Kaletas, R. Dobrawa, A. Sautter, F. Würthner, M. Zimine, L. De Cola, R.M. Williams, J. Phys. Chem. A 108 (2004) 1900.
[18] L. Flamigni, B. Ventura, C.-C. You, C. Hippius, F. Würthner, J. Phys. Chem. C 111 (2007) 622.
[19] S. Xiao, M.E. El-Khouly, Y. Li, Z. Gan, H. Liu, L. Jiang, Y. Araki, O. Ito, D. Zhu, J. Phys. Chem. B 109 (2005) 3658.
[20] W. Seitz, A.J.S. Jimenez, E. Carbonell, B. Grimm, M.S. Rodrıĭguez-Morgade, D.M. Guldi, T. Torres, Chem. Commun. 46 (2010) 127.
[21] E.H.A. Beckers, Z. Chen, S.C.J. Meskers, P. Jonkheijm, A.P.H.J. Schenning, X.-Q. Li, P. Osswald, F. Würthner, R.A.J. Janssen, J. Phys. Chem. B 110 (2006) 16967.
[22] U. Hahn, S. Engmann, C. Oelsner, C. Ehli, D.M. Guldi, T. Torres, J. Am. Chem. Soc. 132 (2010) 6392.
[23] C.-C. You, P. Espindola, C. Hippius, J. Heinze, F. Würthner, Adv. Funct. Mater. 17 (2007) 3764.
[24] S. Fukuzumi, K. Ohkubo, J. Ortiz, A.M. Gutiérrez, F. Fernández-Lázaro, Á. Sastre-Santos, J. Phys. Chem. A 112 (2008) 10744.
[25] F.J. Céspedes-Guirao, K. Ohkubo, S. Fukuzumi, Á. Sastre-Santos, F. Fernández-Lázaro, J. Org. Chem. 74 (2009) 5871.
[26] H. Zollinger (Ed.), Color Chemistry, 3rd ed., VCH, Weinheim, Germany, 2003.
[27] C. Li, M. Liu, N.G. Pschirer, M. Baumgarten, K. Müllen, Chem. Rev. 110 (2010) 6817.
[28] J. Li, F. Dierschke, J. Wu, A.C. Grimsdale, K. Muüllen, J. Mater. Chem. 16 (2006) 96.
[29] R. de Bettignies, Y. Nicolas, P. Blanchard, E. Levillain, J.M. Nunzi, J. Roncali, Adv. Mater. 15 (2003) 1939.
[30] L. Schmidt-Mende, A. Fechtenkotter, K. Müllen, E. Moons, R.H. Friend, J.D. MacKenzie, Science 293 (2001) 1119.
[31] R.F. Kelley, W.S. Shin, B. Rybtchinski, L.E. Sinks, M.R. Wasielewski, J. Am. Chem. Soc. 129 (2007) 3173.
[32] P. Osswald, F. Würthner, Chem. Eur. J. 13 (2007) 7395.
[33] T.E. Kaiser, H. Wang, V. Stepanenko, F. Würthner, Angew. Chem. Int. Ed. 46 (2007) 5541.
[34] R. Schmidt, M.M. Ling, J.H. Oh, M. Winkler, M. Könemann, Z. Bao, F. Würthner, Adv. Mater. 19 (2007) 3692.
[35] J.H. Oh, S. Liu, Z. Bao, R. Schmidt, F. Würthner, Appl. Phys. Lett. 91 (2007) 212107.
[36] P. Jonkheijm, N. Stutzmann, Z. Chen, D.M. de Leeuw, E.W. Meijer, A.P.H.J. Schenning, F. Würthner, J. Am. Chem. Soc. 128 (2006) 9535.
[37] A. Mishra, C-Q. Ma, P. Bäuerle, Chem. Rev. 109 (2009) 1141.
[38] D. Fichou (Ed.), Handbook of Oligo- and Polythiophenes, Wiley-VCH, Weinheim, 1999.
[39] P. Bäuerle, K. Müllen, G. Wegener (Eds.), Electronic Materials: The Oligomer Approach, Wiley-VCH, Weinheim, 1998.
[40] I.F. Perepichka, D.F. Perepichka, H. Meng, F. Wudl, Adv. Mater. 17 (2005) 2281.
[41] B.J. Holliday, T.M. Swager, Chem. Commun. (2005) 23.
[42] H. Rockel, J. Huber, R. Gleiter, W. Schuhmann, Adv. Mater. 6 (1994) 568.
[43] D.M. Welsh, A. Kumar, E.W. Meijer, J.R. Reynolds, Adv. Mater. 11 (1999) 1379.
[44] E. Mena-Osteritz, P. Bäuerle, Adv. Mater. 18 (2006) 447.
[45] F. Jäckel, M.D. Watson, K. Müllen, J.P. Rabe, Phys. Rev. Lett. 92 (2004) 188303.
[46] T. Benincori, V. Bonometti, F. De Angelis, L. Falciola, M. Muccini, P.R. Mussini, T. Pilati, G. Rampinini, S. Rizzo, S. Toffanin, F. Sannicolò, Chem. Eur. J. 16 (2010) 9086.
[47] J. Cremer, P. Bäuerle, Eur. J. Org. Chem. (2005) 3715.
[48] J.L. Segura, R. Goĭmez, R. Blanco, E. Reinold, P. Baäuerle, Chem. Mater. 18 (2006) 2834.
[49] J. Cremer, P. Bäuerle, J. Mater. Chem. 16 (2006) 874.
[50] J. Cremer, E. Mena-Osteritz, N.G. Pschierer, K. Müllen, P. Bäuerle, Org. Biomol. Chem. 3 (2005) 985.
[51] C.-Q. Ma, E. Mena-Osteritz, T. Debaerdemaeker, M.M. Wienk, R.A. Janssen, P. Baäeuerle, Angew. Chem. Int. Ed. 46 (2007) 1679.
[52] X. Zhan, Z. Tan, B. Domercq, Z. An, X. Zhang, S. Barlow, Y. Li, D. Zhu, B. Kippelen, S.R. Marder, J. Am. Chem. Soc. 129 (2007) 7246.
[53] Y. Ie, T. Uto, N. Yamamoto, Y. Aso, Chem. Commun. (2009) 1213.
[54] M.H. Kim, M.J. Cho, K.H. Kim, M.H. Hoang, T.W. Lee, J.-I. Jin, N.S. Kang, J.-W. Yu, D.H. Choi, Org. Electron. 10 (2009) 1429.
[55] M. Fujitsuka, K. Harada, A. Sugimoto, T. Majima, J. Phys. Chem. A 112 (2008) 10193.
[56] M.K.R. Fischer, T.E. Kaiser, F. Würthner, P. Baäuerle, J. Mater. Chem. 19 (2009) 1129.
[57] E.H.A. Beckers, S.C.J. Meskers, A.P.H.J. Schenning, Z. Chen, F. Würthner, R.A.J. Janssen, J. Phys. Chem. A 108 (2004) 6933.
[58] M. Jaggi, C. Blum, B.S. Marti, S.-X. Liu, S. Leutwyler, S. Decurtins, Org. Lett. 12 (2010) 1344.
[59] L.X. Chen, S. Xiao, L. Yu, J. Phys. Chem. B 110 (2006) 11738.
[60] N. Mataga, H. Miyasaka, in: J. Jortner, M. Bixon (Eds.), In Electron Transfer, John Wiley & Sons, New York, 1999, pp. 431–496, Part 2.
[61] B.R. Arnold, S. Farid, J.L. Goodman, I.R. Gould, J. Am. Chem. Soc. 118 (1996) 5482.
[62] M. Supur, M.E. El-Khouly, J.H. Seok, J.H. Kim, K.-Y. Kay, S. Fukuzumi, J. Phys. Chem. C 114 (2010) 10969.
[63] G.J. Kavarnos (Ed.), Fundamental of Photoinduced Electron Transfer, VCH Publishers, Inc., New York, 1993.
[64] The k_{ET} and Φ_{ET} values via the singlet excited PDI were calculated from the relations; $k_{ET} = (1/\tau_f)\text{sample} - (1/\tau_{f0})\text{reference}$ and $\Phi_{ET} = k_{ET}/(1/\tau_f)\text{sample}$; in which τ_{f0} is the lifetime of the PDI reference (6.0 ns).
[65] J.R. Lakowicz (Ed.), Principles of Fluorescence Spectroscopy, 2nd ed., Kluwer Academic/Plenum Publishers, New York, 1999.
[66] T. Förster, Ann. Phys. 55 (1948).
[67] L. Stryer, R.P. Haugland, Proc. Natl. Acad. Sci. U.S.A. (1967) 719.